Supporting Information

Ancillary-ligand-strategy for the improvement of electrochemical sensing towards S-containing amines with ultralow detection limit

Teng Ma,[a] Yizhen Zhao,[a] Xiao Liu,[a] Xingyue He,[a] Bin Lei,[a] Xiaohang Qiu,*[a] Jian-Gong Ma,*[a] and Peng Cheng[a]

[a] Department of Chemistry, Key Laboratory of Advanced Energy Material Chemistry (MOE), Frontiers Science Center for New Organic Matter, and Renewable Energy Conversion and Storage Center (RECAST), College of Chemistry, Nankai University, Tianjin 300071, P. R. China

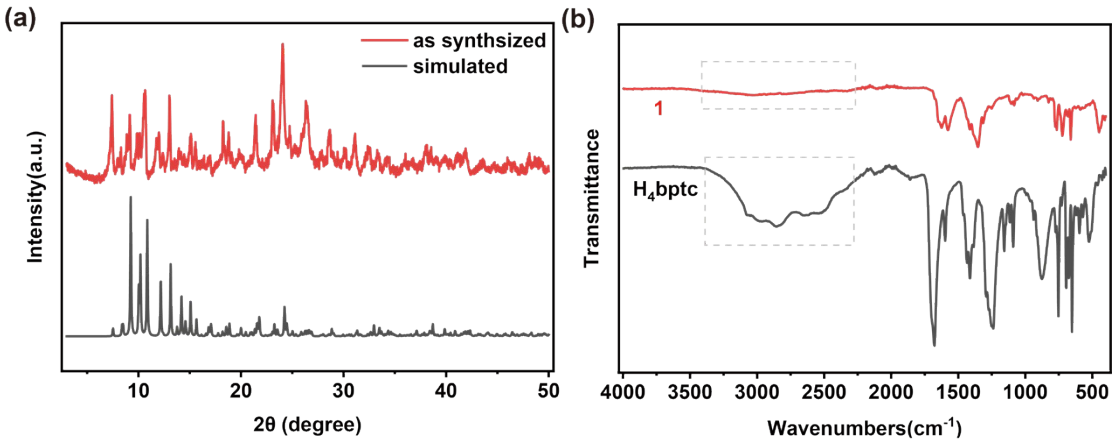

Figure S1 (a) PXRD patterns of **1**. (b) FT-IR spectra of H_4bptc and **1**.

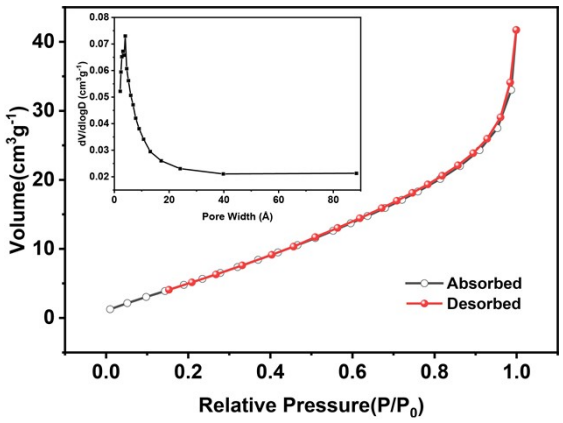

Figure S2 N_2 adsorption–desorption isotherms of **2** at 77 K (inset: the corresponding pore size distribution).

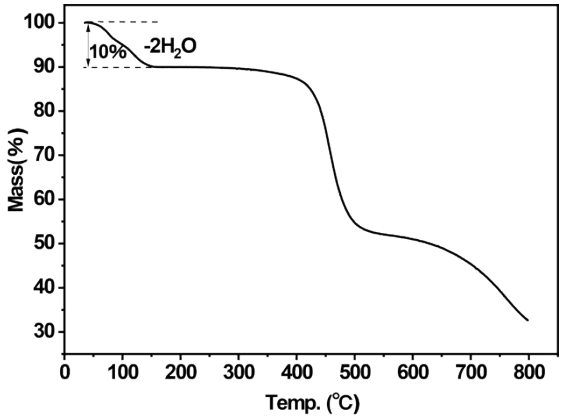

Figure S3 TGA curve of **2**.

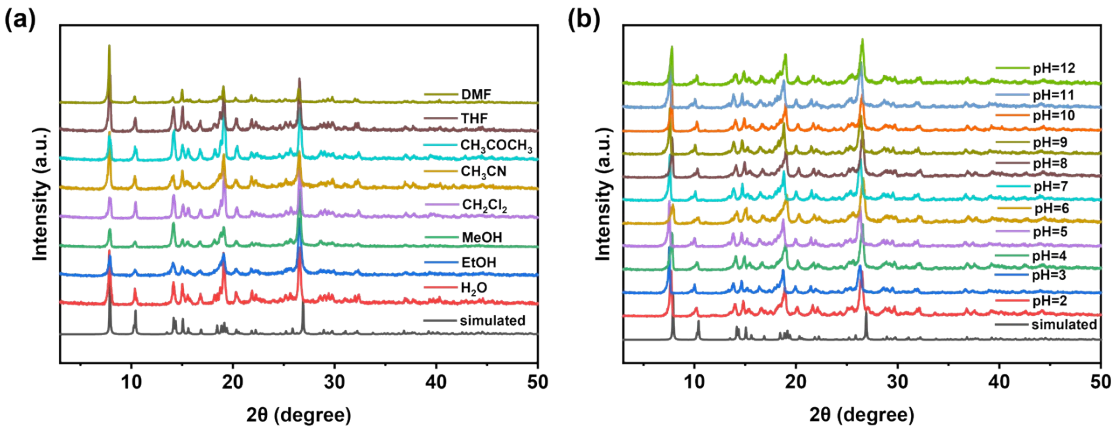

Figure S4 (a) PXRD patterns of **2** after immersing in different solvents for 7d; (b) PXRD patterns of **2** after immersing in water, pH 2 ~ 12 for 7d.

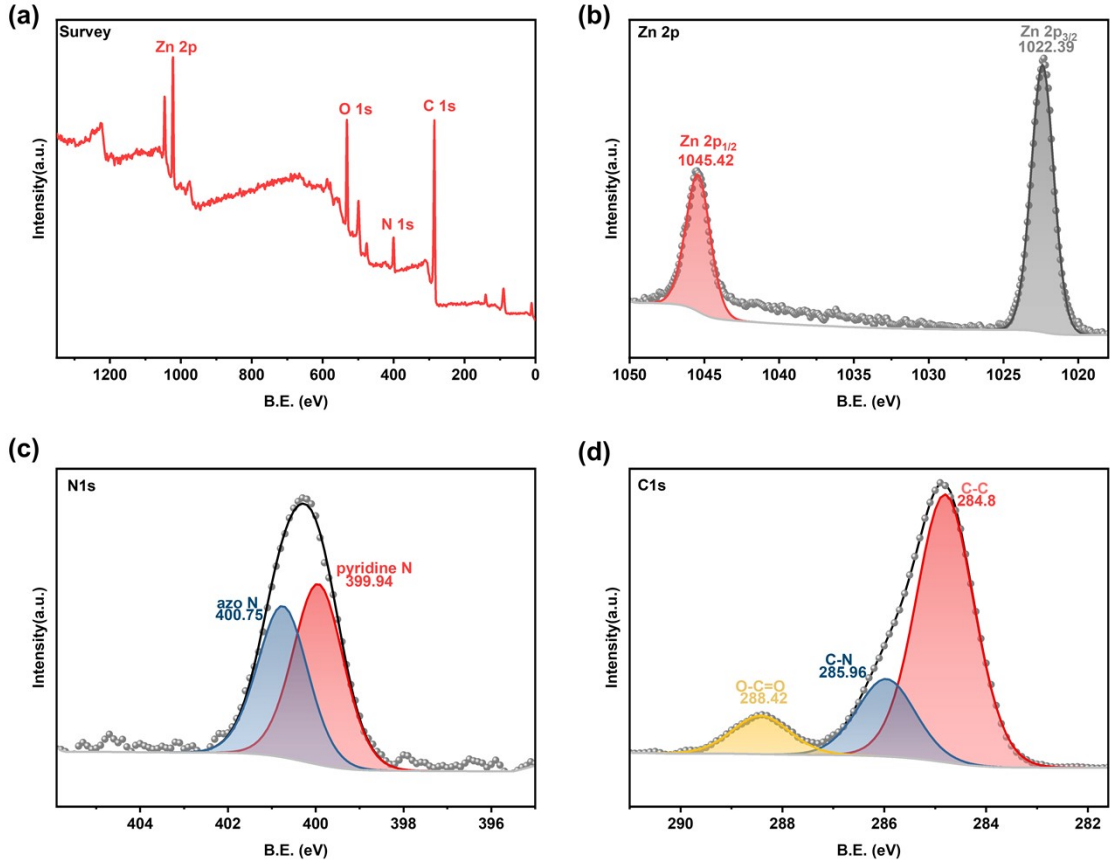

Figure S5 XPS spectra of (a) survey of **2**; (b) Zn 2p; (c) N1s; (d) C1s.

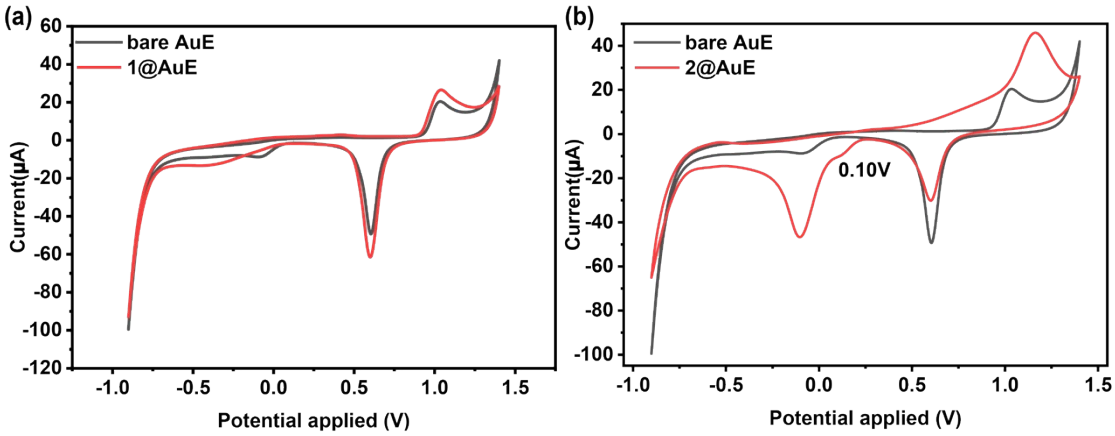

Figure S6 CV characterization of the intrinsic electrochemical activity of **1** and **2** in ABS buffer solution at pH 4.4.

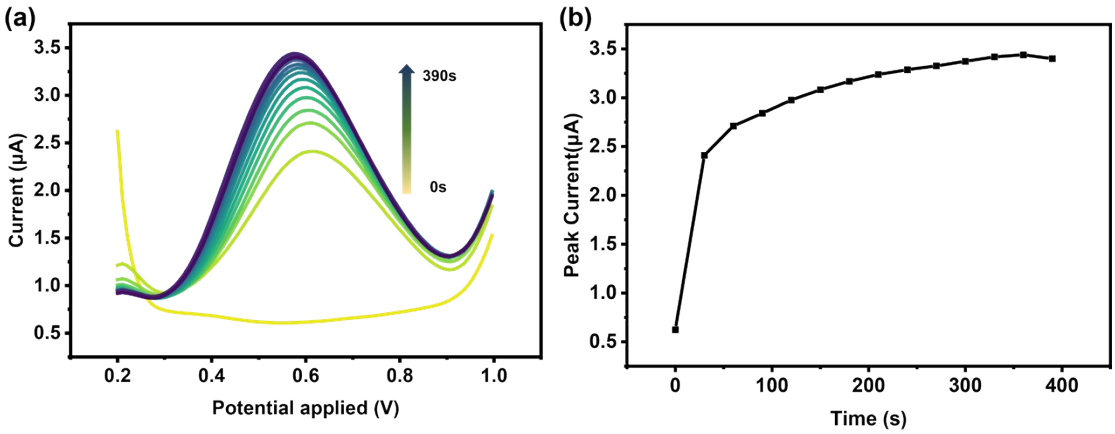

Figure S7 (a) DPV curves of 20 μM L-Met on **2**@AuE in ABS buffer with different accumulation time (0 ~ 390s) (b) The relationship between the oxidation currents of L-Met and accumulation time.

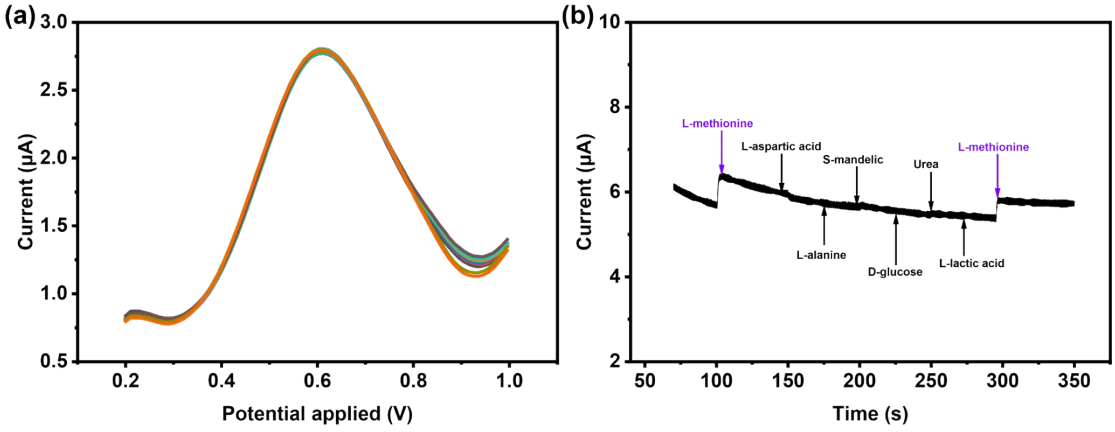

Figure S8 (a) recyclability and (b) selectivity of **2**@AuE towards L-Met.

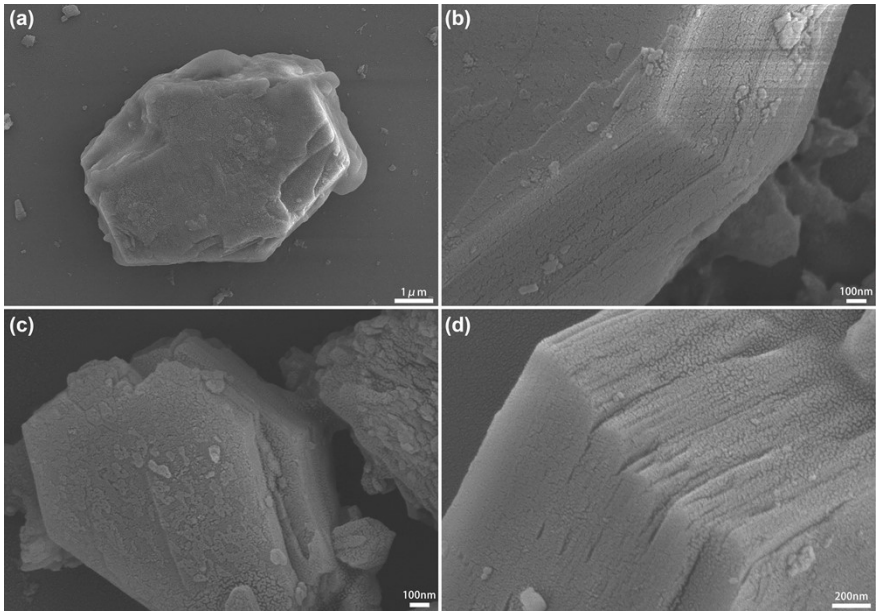

Figure S9 The SEM images of **2** after electrochemical sensing(a, b) and 6 recycle sensing work(c, d) towards L-Met.

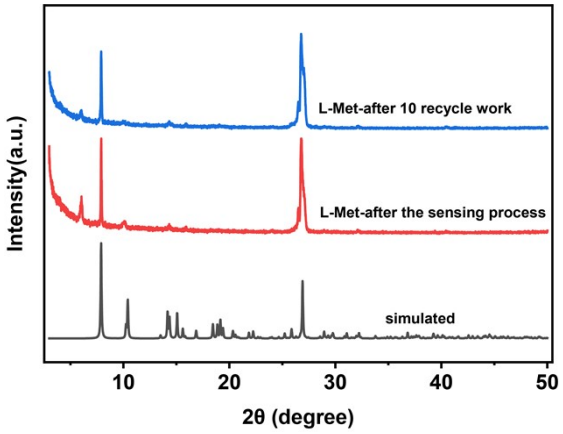

Figure S10 PXRD patterns of **2** after the sensing process and 6 recycle work towards L-Met.

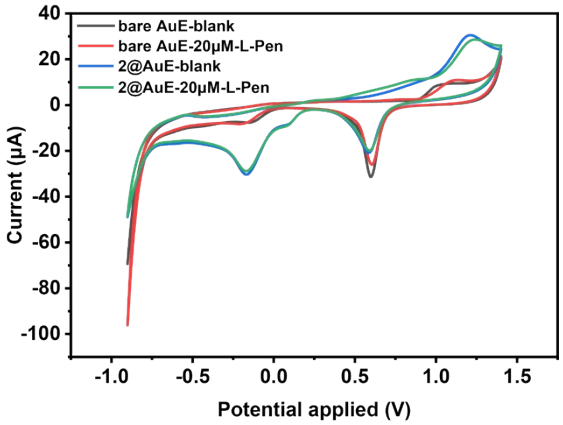

Figure S11 Comparison of CV curves of **2**@AuE and bare AuE in the presence and absence of 20

μM L-Pen in ABS buffer at pH 4.8.

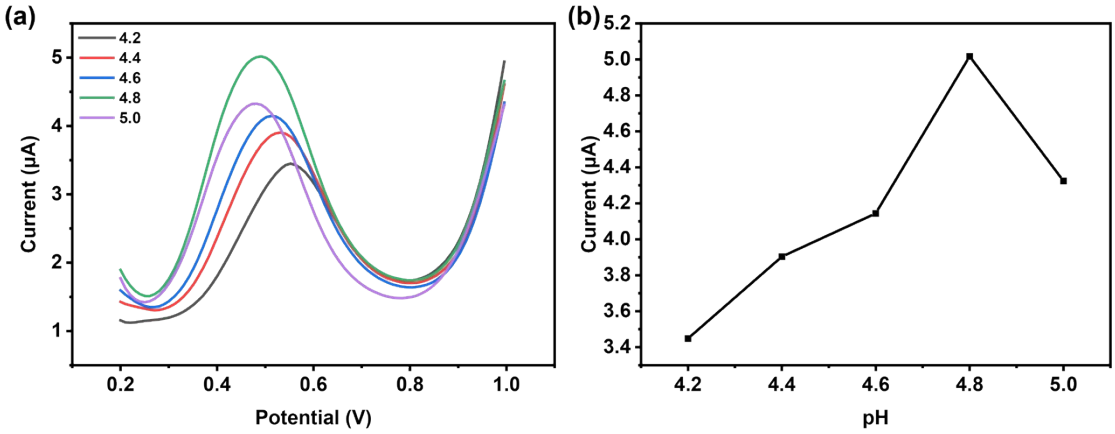

Figure S12 (a) CV curves of 50 μM L-Pen on **2**@AuE in ABS buffer with different pH (4.2–5.0). (b) The relationship between the oxidation currents of L-Pen and pH values.

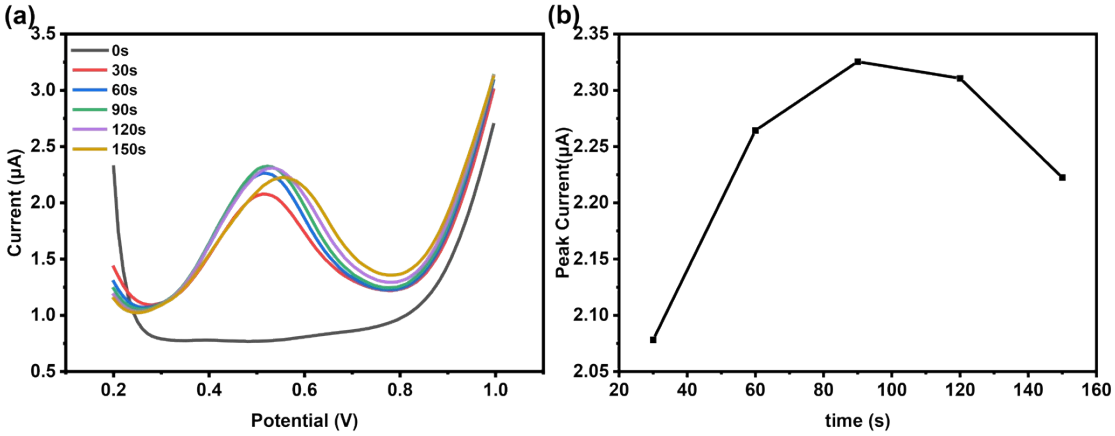

Figure S13 (a) DPV curves of 50 μM L-Pen on **2**@AuE in ABS buffer with different accumulation time (0 ~ 150s) (b) The relationship between the oxidation currents of L-Pen and accumulation time.

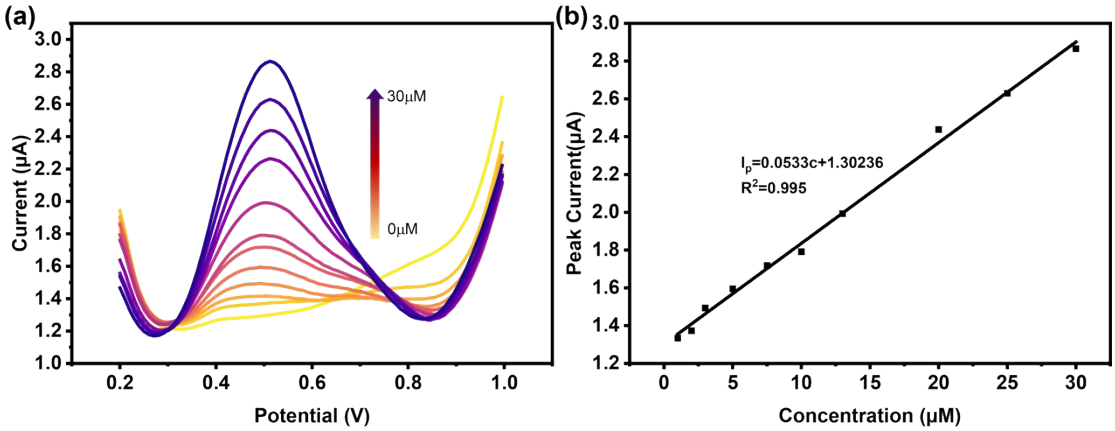

Figure S14 (a) DPV curves of different concentrations of L-Pen on **2**@AuE; (b) Linear relationship between the concentration of L-Pen and oxidation peak current.

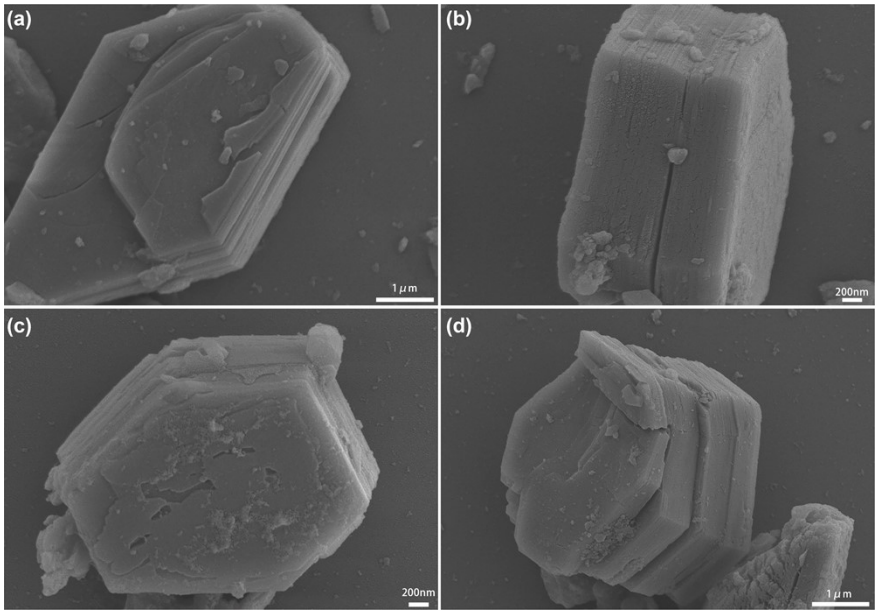

Figure S15 The SEM images of **2** after electrochemical sensing(a, b) and 6 recycle sensing work(c, d) towards L-Pen.

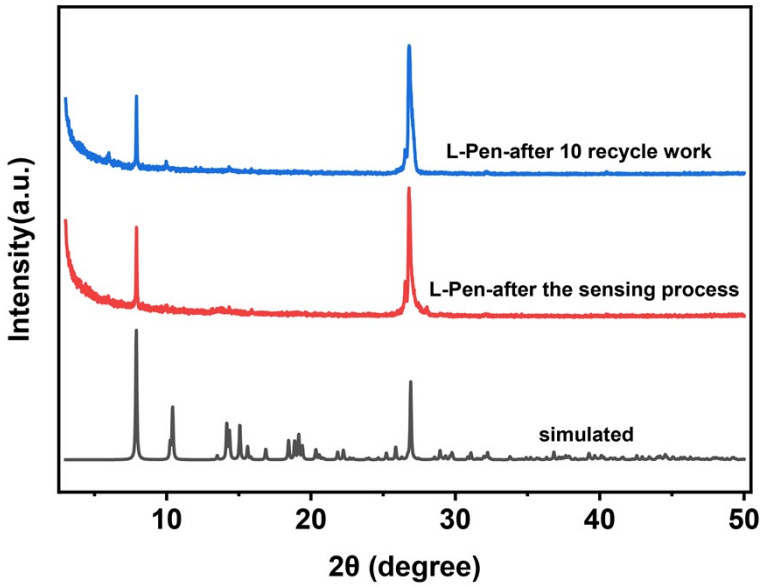

Figure S16 PXRD patterns of **2** after the sensing process and 6 recycle work towards L-Pen.

Table S1 Crystal data and structure refinement for **1**.

Identification code	**1**
CCDC number	2297489
Empirical formula	$C_{22}H_{22}N_2O_{11}Zn_2$
Formula weight	621.15
Temperature/K	100.01(10)
Crystal system	monoclinic
Space group	$P2_1/c$

a/Å	14.3500(2)
b/Å	12.8566(2)
c/Å	21.5209(2)
α/°	90
β/°	125.0700(10)
γ/°	90
Volume/Å^3	3249.61(8)
Z	4
ρ_{calc}g/cm^3	1.270
μ/mm^{-1}	2.248
F(000)	1264.0
Reflections collected	24541
R_{int}	0.0428
GOF on F^2	1.170
R_1, wR_2 [I>=2σ (I)]	0.0583, 0.1401
R_1, wR_2 [all data]	0.0585, 0.1402
Largest diff. peak/hole / e Å^{-3}	1.37/-0.60

Table S2 Crystal data and structure refinement for **2**.

dentification code	**2**
CCDC number	2297488
Empirical formula	$C_{26}H_{18}N_4O_{10}Zn_2$
Formula weight	677.18
Temperature/K	133.6(3)
Crystal system	triclinic
Space group	$P\bar{1}$
a/Å	6.9201(15)
b/Å	9.6208(11)
c/Å	12.0479(10)
α/°	109.196(9)
β/°	94.448(12)
γ/°	105.662(14)
Volume/Å^3	717.1(2)
Z	1
ρ_{calc}g/cm^3	1.568
μ/mm^{-1}	1.734
F(000)	342.0
Reflections collected	5191
Rint	0.0677
GOF on F^2	0.973
R_1, wR_2 [I>=2σ (I)]	0.0743, 0.1199
R_1, wR_2 [all data]	0.1387, 0.1506
Largest diff. peak/hole / e Å$^-$	0.67/-0.83

3	

Table S3 The comparison of **2**@AuE with other electrode for electrochemical sensing of L-Met.

Working Electrode	Linear range (μM)	Limit of detection (μM)	Sensitivity (μA mM^{-1} cm^{-2})	Ref
2	0.05~1 μM and 1~30 μM	6.4×10^{-6} μM	3.637 μA μM^{-1} cm^{-2} (0.05~1 μM) and 10.706 μA μM^{-1} cm^{-2} (1~30 μM)	This work
3D PLA-GNaOH-EC electrode	5.0 μM – 3000 μM	1.39μM	0.176 μAL μmol^{-1}	[1]
GC/GCN−S electrode	0.1μM to 200 μM	3.2×10^{-4} μM	1.16 μA μM^{-1} cm^{-2}	[2]
Mn_2O_3/SPCE	1.0 to 6.1 μM	1.0×10^{-3} μM	6.036 (±0.002) μA μM^{-1} cm^{-2}	[3]
MnO_2@MnCeO	1000–10000 and 1–750 μM	0.16 μM	-	[4]
AgO modified graphite pencil electrode	60 μM - 500 μM	0.42 μM	4.23 μA μM^{-1} cm^{-2}	[5]

Reference:

1. C. Kalinke, N. V. Neumsteir, P. Roberto de Oliveira, B. C. Janegitz and J. A. Bonacin, *Anal. Chim. Acta*, 2021, **1142**, 135-142.
2. A. Ajith and S. A. John, *Electroanal*, 2023, **35**, e202200063.
3. R. Sasikumar, T. W. Chen, S. M. Chen, S. P. Rwei and M. C. Yu, *Int. J. Electrochem. Sci.*, 2018, **13**, 4561-4574.
4. M. Rashedi and T. Alizadeh, *J. Electrochem. Soc.*, 2023, **170**, 017502.
5. N. A. Odewunmi, A. N. Kawde and M. Ibrahim, *Sens. Actuators, B*, 2019, **281**, 765-773.